Oncogene (2017) **36**, 4288–4298

www.nature.com/onc

OPEN

ORIGINAL ARTICLE

SerpinB2 regulates stromal remodelling and local invasion in pancreatic cancer

NLE Harris[1,2,3,9], C Vennin[4,5,9], JRW Conway[4,5], KL Vine[1,2,3], M Pinese[4], MJ Cowley[4], RF Shearer[4,5], MC Lucas[4,5], D Herrmann[4,5], AH Allam[4], M Pajic[4,5], JP Morton[6], Australian Pancreatic Cancer Genome Initiative, AV Biankin[7], M Ranson[1,2,3], P Timpson[4,5] and DN Saunders[4,8]

Pancreatic cancer has a devastating prognosis, with an overall 5-year survival rate of ~8%, restricted treatment options and characteristic molecular heterogeneity. SerpinB2 expression, particularly in the stromal compartment, is associated with reduced metastasis and prolonged survival in pancreatic ductal adenocarcinoma (PDAC) and our genomic analysis revealed that SERPINB2 is frequently deleted in PDAC. We show that SerpinB2 is required by stromal cells for normal collagen remodelling *in vitro*, regulating fibroblast interaction and engagement with collagen in the contracting matrix. In a pancreatic cancer allograft model, co-injection of PDAC cancer cells and SerpinB2$^{-/-}$ mouse embryonic fibroblasts (MEFs) resulted in increased tumour growth, aberrant remodelling of the extracellular matrix (ECM) and increased local invasion from the primary tumour. These tumours also displayed elevated proteolytic activity of the primary biochemical target of SerpinB2—urokinase plasminogen activator (uPA). In a large cohort of patients with resected PDAC, we show that increasing uPA mRNA expression was significantly associated with poorer survival following pancreatectomy. This study establishes a novel role for SerpinB2 in the stromal compartment in PDAC invasion through regulation of stromal remodelling and highlights the SerpinB2/uPA axis for further investigation as a potential therapeutic target in pancreatic cancer.

Oncogene (2017) **36,** 4288–4298; doi:10.1038/onc.2017.63; published online 27 March 2017

INTRODUCTION

Pancreatic ductal adenocarcinoma (PDAC) represents ~92% of all pancreatic cancers and is one of the deadliest of all solid malignancies, with a 5-year survival rate of 8%.[1] PDAC is often resistant to therapy owing to intrinsic chemoresistance, hypovascularity and an extensive desmoplastic reaction that creates a barrier of fibrotic tissue preventing drug penetration.[2] As a result, established approaches to pancreatic cancer therapy (that is surgical resection and Gemcitabine/Abraxane treatment)[3,4] show low efficacy—with only 25–30% of patients responding[5]—and have limited impact on metastatic disease. Aside from frequent K-Ras mutations (>90% of tumours), we have shown that PDAC is characterized by a high degree of molecular heterogeneity, making identification of suitable candidates for targeted therapy challenging.[6–8] Advances in adjuvant and metastatic chemotherapeutic regimens have resulted in modest improvements in outcome; however, pancreatectomy remains the single most effective and the only potentially curative modality for the ~20% of patients suitable for such a procedure.

PDAC is characterized by a significant abundance of activated fibroblasts and other stromal cells such as stellate cells, and these have been implicated as major facilitators of disease progression,[9–14] where reduced stromal integrity is associated with enhanced tumour growth, invasion and metastasis. Despite this increased interest, our understanding of tumour-stromal interactions in PDAC remains relatively poor and is likely hindering the development of effective therapies.

The plasminogen activation system (PAS) plays a key role in tumour invasion and metastasis—increasing the capacity to breakdown tissue barriers through generation of the proteolytic enzyme plasmin by tumour and stromal cells.[15] The main activator of the PAS is the serine protease urokinase (urokinase plasminogen activator (uPA)). Overexpression of uPA is an important biomarker of metastatic disease and it is being actively investigated as a therapeutic target.[15–17] Upon binding to its cellular receptor, uPAR, the pro-uPA zymogen is catalytically converted into its active form, which in turn activates co-localized plasminogen into the broad-spectrum protease, plasmin. The combined signalling and proteolytic outputs of this pathway activate a plethora of downstream events driving extracellular matrix (ECM) degradation, cell proliferation, adhesion and migration.[18] Negative regulation of this pathway occurs at several levels, including inhibition and clearance of protease activity by naturally occurring inhibitors, such as SerpinB2 and SerpinE1 (Plasminogen Activator Inhibitors, PAI-2 and PAI-1, respectively).[15,19] Elevated SerpinB2 expression has been linked with prolonged survival, decreased metastasis or decreased tumour growth in a number of cancer types,[15] including three small-scale studies in human PDAC.[20,21]

[1]Illawarra Health and Medical Research Institute, University of Wollongong, Wollongong, Australia; [2]Centre for Medical and Molecular Bioscience, University of Wollongong, Wollongong, Australia; [3]School of Biological Sciences, University of Wollongong, Wollongong, Australia; [4]Kinghorn Cancer Center, Garvan Institute of Medical Research, Darlinghurst, Australia; [5]St Vincent's Clinical School, Faculty of Medicine, University of New South Wales, Darlinghurst, Australia; [6]Cancer Research UK Beatson Institute, Glasgow, Scotland; [7]Wolfson Wohl Cancer Research Centre, Institute of Cancer Sciences, University of Glasgow, Glasgow, UK and [8]School of Medical Sciences, University of New South Wales, Sydney, Australia. Correspondence: Professor M Ranson, Illawarra Health and Medical Research Institute, Building 32, Northfields Ave, Wollongong, NSW, 2522, Australia or Dr P Timpson, The Kinghorn Cancer Centre, Garvan Institute of Medical Research, Victoria St, Darlinghurst, NSW, 2010. Australia or Dr D Saunders, School of Medical Sciences, UNSW Australia, Sydney, NSW, 2052, Australia.

E-mail: mranson@uow.edu.au or p.timpson@garvan.org.au or d.saunders@unsw.edu.au

[9]These authors contributed equally to this work.

Received 16 August 2016; revised 11 January 2017; accepted 8 February 2017; published online 27 March 2017

Even though SerpinB2 is clearly implicated in PDAC progression, cell-specific studies have yet to be undertaken to understand the role of SerpinB2 in specific cell compartments. For example, SerpinB2 expression in oesophageal squamous cell carcinoma-associated fibroblasts correlated with prolonged patient survival.[22] Furthermore, analysis of expression array data from isolated human breast tumours and matched normal stroma[23] identified a significant (~16x; $P < 0.0001$) reduction in SerpinB2 expression in stroma from invasive carcinoma compared with normal breast. Only a few clinical studies have looked closely at cell-specific expression in human PDAC,[24–26] with varying results that may be confounded by limited sample sizes. Given these limitations, we applied 3D organotypic culture[27–30] and *in vivo* allografts using cells from a mouse model of pancreatic cancer (*Pdx1-Cre, LSL-KRas$^{G12D/+}$, LSL-Trp53$^{R172H/+}$*, KPC model) that closely recapitulate the human disease,[31–33] and SerpinB2 deficiency,[34] to investigate the role of SerpinB2 in the PDAC tumour microenvironment. Using these models we demonstrate that SerpinB2 regulates stromal remodelling of collagen, in turn influencing tumour growth and invasion.

RESULTS

Frequent genomic alterations of plasminogen activation system genes in PDAC

In the specific context of pancreatic cancer, expression of various individual components of the PAS has been associated with differential survival or outcome in a small cohort of PDAC patients.[24,26] Across a panel of cancer types, genomic alterations of PAS component genes (SERPINB2, PLAU, PLAUR, SERPINE1) were most frequently observed in a PDAC cohort (University of Texas - Southwestern (UTSW) cohort,[35] 42% of 109 cases, Figure 1a), with deep deletion of SERPINB2 in 24% of these cases. Interestingly, genomic alterations of either the enzyme (PLAU), receptor (PLAUR) or inhibitors (SERPINB2, SERPINE1) of the PAS pathway appeared to be mutually exclusive in PDAC (Figure 1b). These data highlight the potential importance of the PAS system, in particular loss of SerpinB2, in PDAC.

Stromal SerpinB2 is necessary for fibroblast-contracted collagen I matrix formation and integrity during ECM remodelling

Stromal expression of SerpinB2 has been linked to progression in a number of tumour types.[15] To investigate the role of stromal SerpinB2 in the regulation of PDAC stromal remodelling, we used wild-type or SerpinB2$^{-/-}$ mouse embryonic fibroblasts (MEFs) to drive collagen contraction *in vitro*. Interestingly, collagen matrices formed by SerpinB2$^{-/-}$ MEFs showed significant structural differences to those generated by wild-type MEFs (Figure 2). After a 12-day contraction period wild-type MEF-contracted collagen I matrices were on average 2.3x smaller than those contracted by SerpinB2$^{-/-}$ MEFs (Figure 2a and b), corresponding to a 58% reduction in the rate of matrix contraction in the absence of SerpinB2 (Figure 2b). Second harmonic generation (SHG) imaging is a label-free, two photon microscopy technique used to image fibrillar, crosslinked collagen in tissue. SHG analysis of fibrillar collagen after the 12-day contraction period showed a significant decrease in fibrillar collagen in the absence of SerpinB2 (Figures 2c–e; Supplementary Movies S1–S4). In wild-type matrices, maximum SHG intensity signal was 31.58 (s.e.m. = 3.84) while maximum SHG signal only reached 11.39 (s.e.m. = 1.34) in SerpinB2$^{-/-}$ matrices (Figure 2e; Supplementary Movie S5). Similar results were observed using a second, independently derived set of wild-type and SerpinB2$^{-/-}$ MEF isolates (Supplementary Figure S4), indicating that additional variant factors do not contribute to these differences in matrix contraction rates and integrity. Scanning electron microscopy (SEM) imaging showed extensive fibril

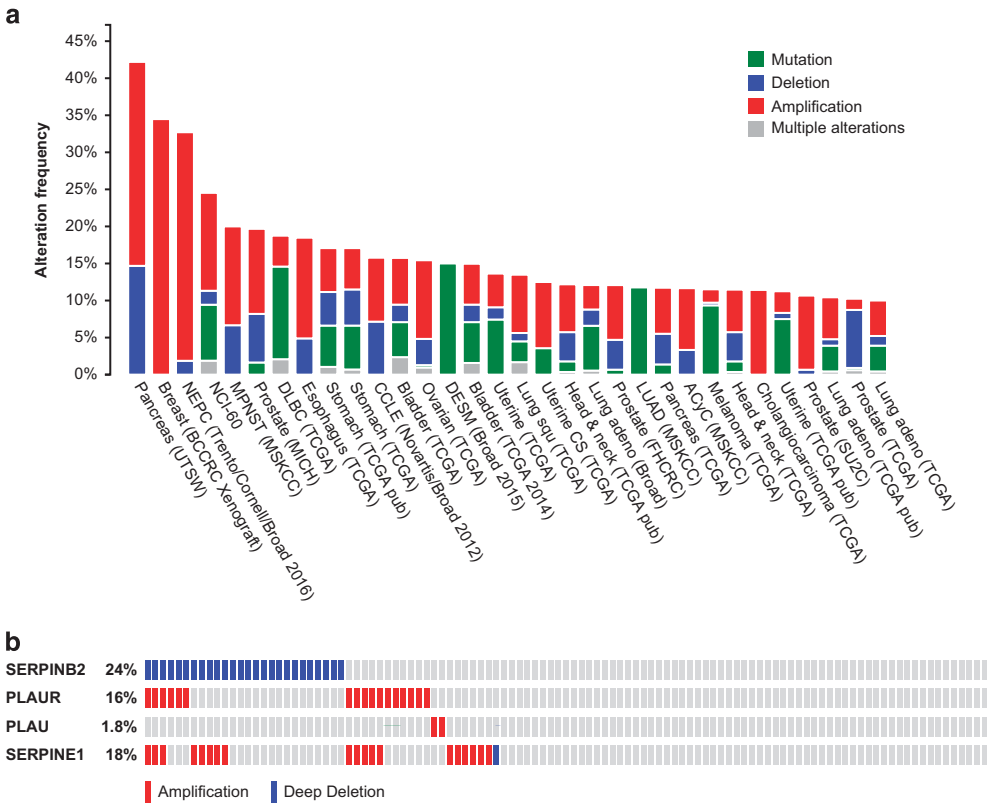

Figure 1. The SERPINB2 gene is frequently deleted in PDAC. (**a**) Alteration frequencies of the PAS component genes SERPINB2, PLAU, PLAUR and SERPINE1 across various cancer types in the cBIO cancer genomics database. (**b**) Oncoprint showing mutual exclusivity of SERPINB2 PLAU, PLAUR and SERPINE1 genomic alterations in pancreatic tumours in the UTSW dataset ($n = 109$).

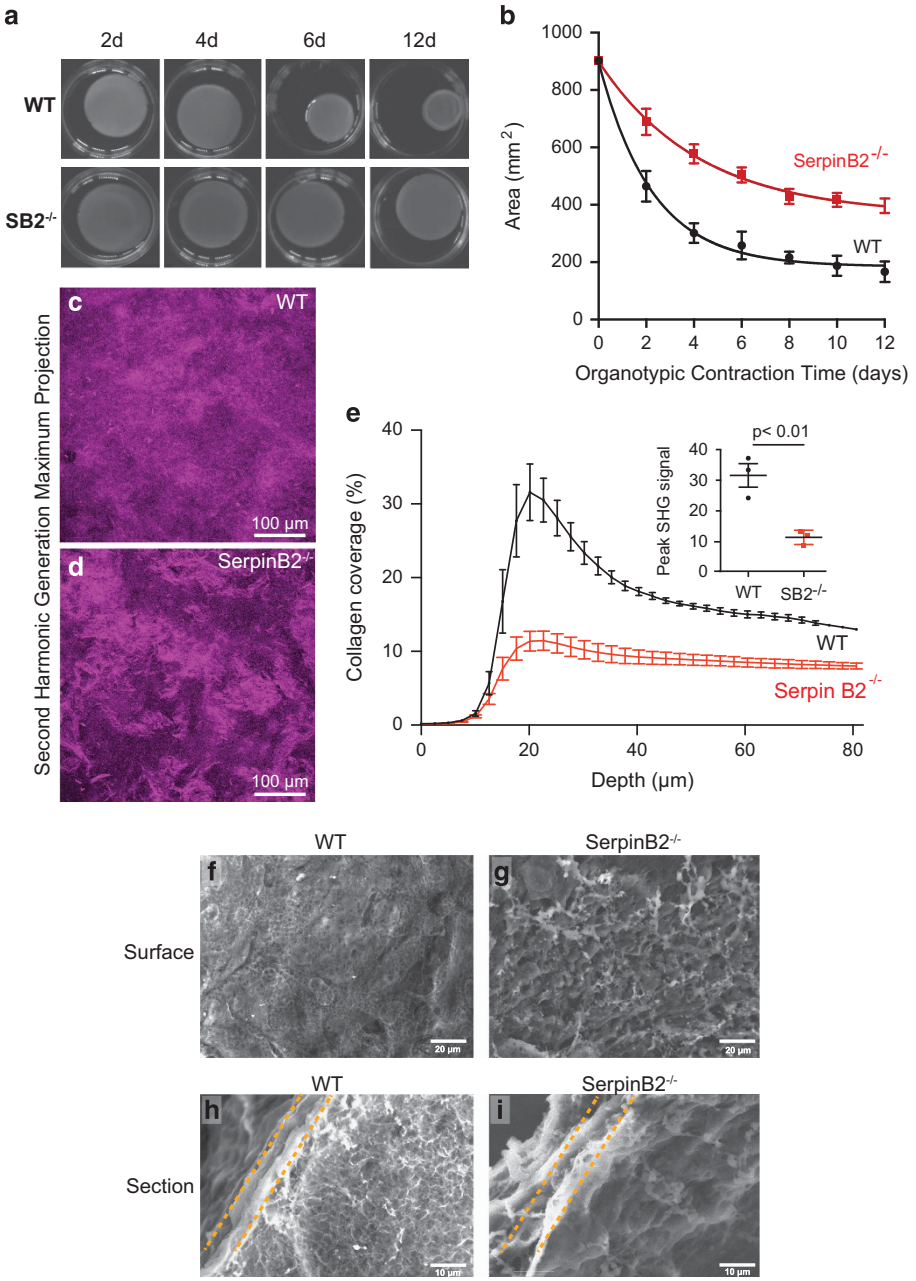

Figure 2. Fibroblast-derived SerpinB2 is necessary for efficient collagen I matrix contraction. (**a**) Photographs showing collagen I matrix contraction over 12 days in the presence of either wild-type or SerpinB2$^{-/-}$ MEFs. (**b**) Changes in area (mm^2) of collagen matrices shown in (**a**) over the 12-day contraction period. (**c**, **d**): Maximum projection through 0–80 µm z-stack of SHG signal intensity of collagen I matrices formed with either (**c**) wild-type or (**d**) SerpinB2$^{-/-}$ MEFs (**e**) Quantification of SHG signal intensity within matrices formed by either wild-type or SerpinB2$^{-/-}$ MEFs, inset: mean SHG signal peak. (**f**–**i**) SEM ultrastructure analysis showing surface (**f**, **g**) or sagittal section (**h**, **i**) of collagen I matrices. Values shown are mean ± s.e.m. from three separate experiments, statistical analysis performed using an unpaired *t*-test.

coverage, robust outer matrix structure and homogenous, isotropic collagen distribution in wild-type matrices (Figures 2f and h). Conversely, SerpinB2$^{-/-}$ MEFs formed disordered, anisotropic collagen networks, with SEM revealing dense collagen bundles distributed in an unregulated fashion and resulting in poor collagen network integrity (Figures 2g and i). Hence, expression of SerpinB2 in stromal cells is required for collagen remodelling *in vitro*.

In order to further understand the effect of SerpinB2 on matrix contraction, live imaging of collagen remodelling by green fluorescent protein (GFP)-labelled fibroblasts was performed at day 6 of contraction and over a 14-h period. We observed significant differences in the morphology and behaviour of wild-type versus SerpinB2$^{-/-}$ MEFs (Figure 3a). Wild-type MEFs appeared more spread out and were highly mobile, moving freely throughout the matrix, while SerpinB2$^{-/-}$ MEFs were significantly less mobile (Figures 3b–d; Supplementary Movie S6). Notably, wild-type MEFs were predominantly multipolar, with dynamic cycling of numerous and short protrusions. In contrast, SerpinB2$^{-/-}$ MEFs were predominately bipolar—with fewer but longer and more stable protrusions observed (Figures 3e and f). Hence, the ability of MEFs to stably interact and engage with collagen within the contracting collagen matrix is significantly

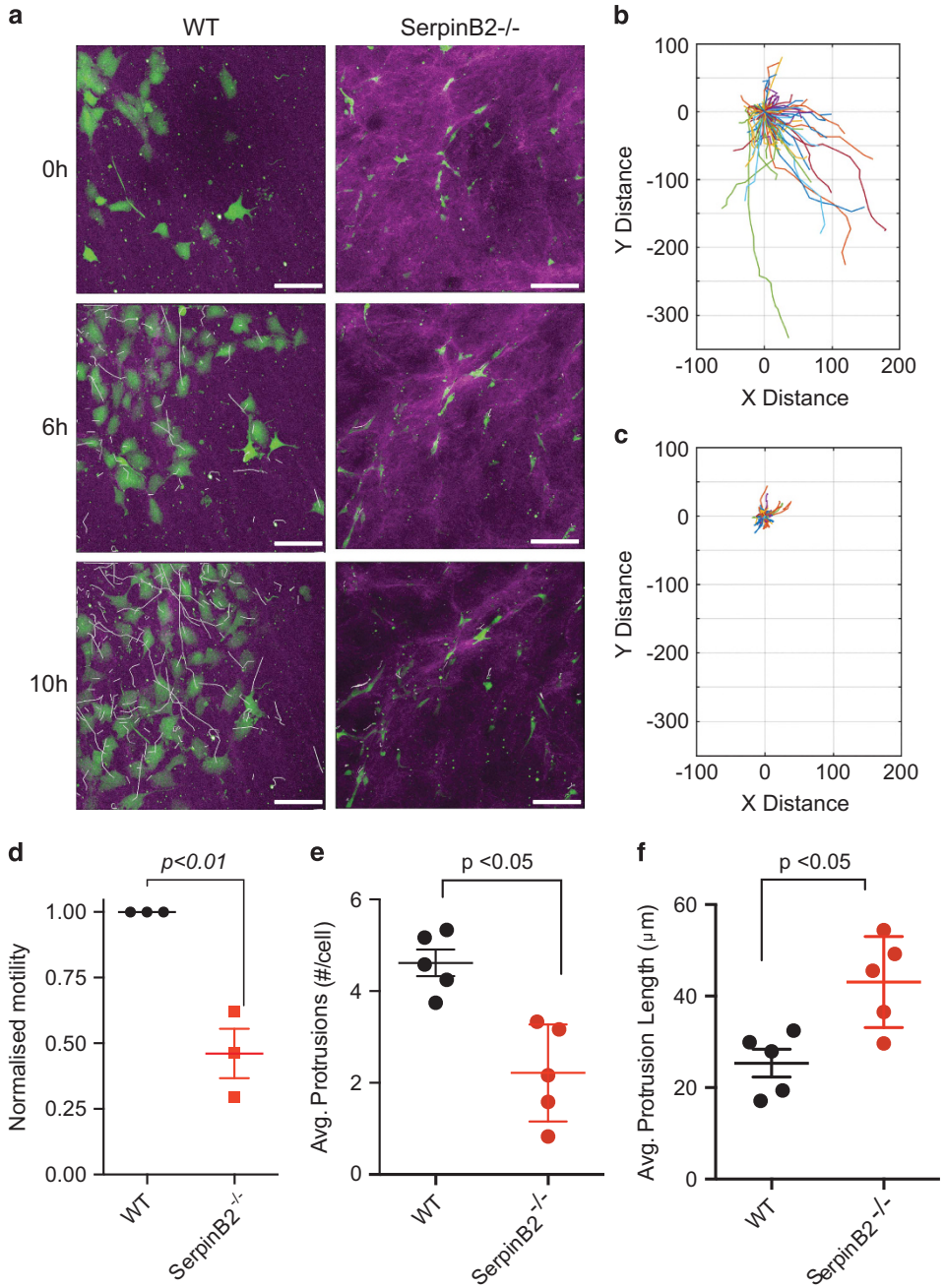

Figure 3. SerpinB2 is necessary for efficient migration of MEFs during collagen I matrix contraction. (**a**) Migration of wild-type or SerpinB2$^{-/-}$ MEFs through collagen I matrices was tracked over 14 h at day 6 of contraction. Collagen (magenta) was detected using SHG and wild-type or SerpinB2$^{-/-}$ MEFs were detected through stable GFP expression. Cell tracks are marked by a vector tail (white). (**b**, **c**) Polar plots denoting cell directionality (x,y distance) and total displacement (μm) of either wild-type (**b**) or SerpinB2$^{-/-}$ (**c**) MEFs through collagen I matrices over the time course (14 h) of the experiment. (**d**) Normalized motility of wild-type or SerpinB2$^{-/-}$ MEFs through collagen I matrices was computed by tracking cell position over time (mean ± s.em. from three separate matrices). (**e**) Average number of protrusions per cell over time (mean ± s.e.m. across five time points). (**f**) Average length of protrusions per cell across the course of the experiment (mean ± s.e.m. across five time points). Statistical analyses were performed using unpaired *t*-tests.

modified in the absence of SerpinB2, and this altered behaviour is likely responsible for the observed structural changes in matrix formed by SerpinB2$^{-/-}$ MEFs (Figure 2).

Stromal SerpinB2 suppresses PDAC tumour growth and local invasion in mixed cell allografts

To determine the effects of modulating SerpinB2 expression in the stroma *in vivo*, we performed an allograft experiment where PDAC cells and MEFs (wild-type or SerpinB2$^{-/-}$) were co-injected into nude mice (Figure 4a). We used a MEF:PDAC ratio of 3:1 to reflect the high fibroblast content and low tumour cellularity of PDAC tumours.[36–38] Seven days post inoculation (see imaging schedule —Figure 4a), PDAC tumours formed with SerpinB2$^{-/-}$ MEFs were larger and more elongated than those formed with wild-type MEFs (mean length 9.7 mm ± 0.5 versus 7.8 mm ± 0.7, respectively, Figure 4b). IHC analysis of tumour cell proliferation showed significantly elevated Ki-67 staining in tumour cells

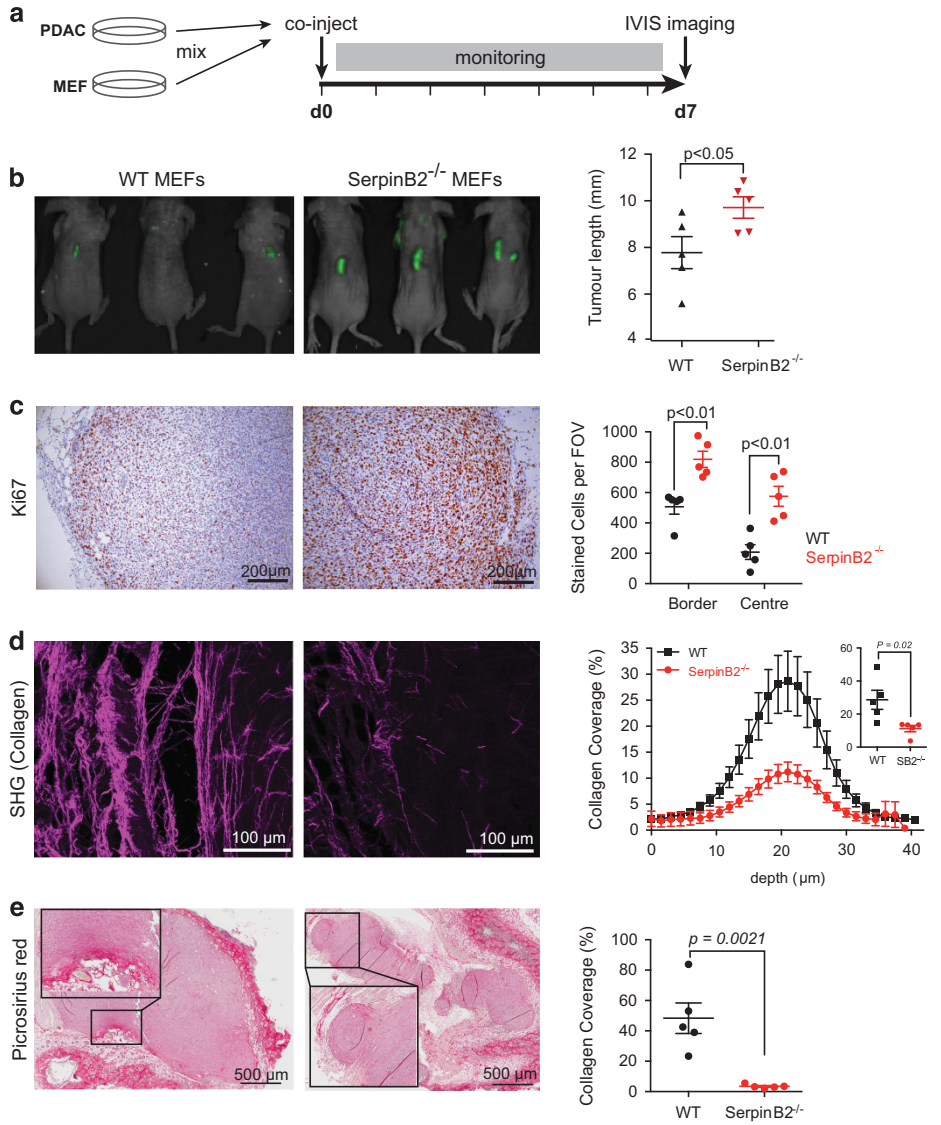

Figure 4. Stromal SerpinB2 attenuates PDAC tumour growth in mixed cell allografts. (**a**) A mixture of MEFs (wild-type or SerpinB2$^{-/-}$) and PDAC cells (at a 3:1 MEF:PDAC ratio) were inoculated s.c. into nude mice and allowed to grow for 7 days prior to euthanasia and tissue collection. (**b**) IVIS imaging of MEF-GFP fluorescence; tumour volume quantification (mean ± s.e.m., $n = 5$). (**c**) Ki-67 staining and quantification at both the border and centre of tumours (with insets showing high magnification view). (**d**) Maximum projection of SHG signal intensity within MEF:PDAC tumours and quantification of SHG signal (inset shows intensity of SHG signal peak). (**e**) Picrosirius staining (with insets showing high magnification view) and quantification of collagen I/III coverage of tumours. Individual values shown are means from three representative images per tumour, from five animals per group with mean ± s.e.m. denoted. Statistical analyses were performed using unpaired *t*-tests.

of the SerpinB2$^{-/-}$ MEF tumours compared to those formed with wild-type MEFs (tumour border = 819 ± 53.3 versus 506 ± 48.1 positive cells per field of view, $P < 0.01$; tumour centre = 576 ± 65.7 versus 208 ± 48.2 positive cells per field of view, $P < 0.01$; Figure 4c).

Consistent with *in vitro* experiments, we also observed significant changes in collagen matrix remodelling of allograft tumours in the absence of stromal SerpinB2. SHG analysis (Figure 4d) showed a significant decrease in collagen content at tumour margins in the absence of MEF SerpinB2 (mean SHG signal intensity 28.7 ± 5.8 versus 11.2 ± 1.9 in wild-type versus SerpinB2$^{-/-}$ MEFs, respectively; $P = 0.02$). Quantification of collagen I and III content in allografts by picrosirius red staining (Figure 4e) revealed significantly decreased collagen coverage in tumours formed with SerpinB2$^{-/-}$ MEFs compared to wild-type (48.4 ± 10.1% versus 3.5 ± 0.6%, respectively; $P = 0.0021$).

Examination of allograft tumour margins by immunofluorescence (Supplementary Figure S2) showed that many cells were positive for alpha-smooth muscle actin, marking activated fibroblasts, which are known to influence tumour progression and invasion.[39] This analysis also showed significantly higher expression of uPA in tumours formed with SerpinB2$^{-/-}$ MEFs compared to those formed with wild-type MEFs (Supplementary Figure S2A). Furthermore, uPA antigen distribution appears to be localized to discrete regions within tumours formed with wild-type MEFs, with a more homogenous distribution observed in tumours formed with SerpinB2$^{-/-}$ MEFs (Supplementary Figure S2A). As expected, while some cells showed clear expression of SerpinB2 in tumours formed with wild-type MEFs, very little SerpinB2 was detected in tumours from SerpinB2$^{-/-}$ MEFs (Supplementary Figure S2B).

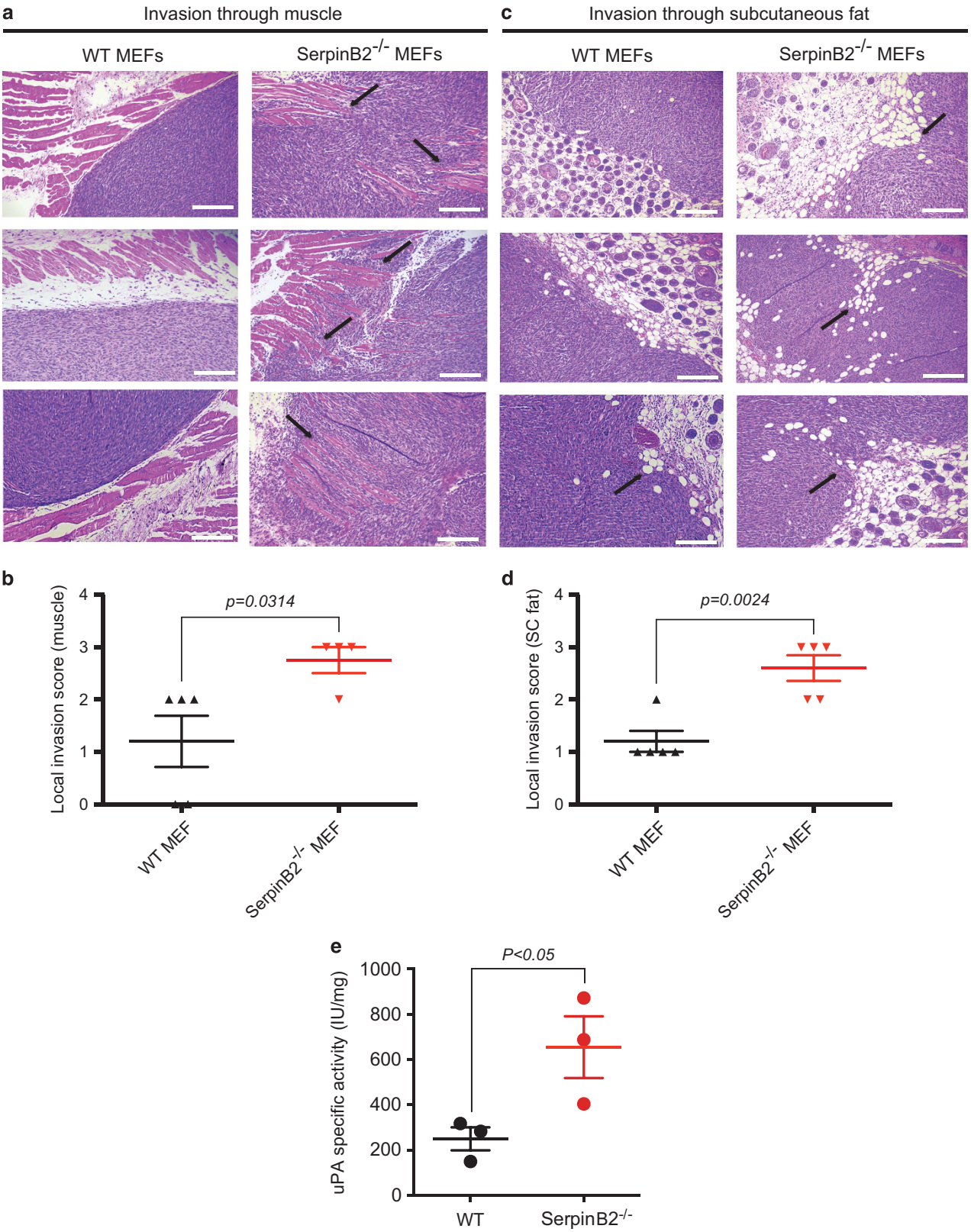

Figure 5. Stromal SerpinB2 attenuates PDAC local invasion in mixed cell allografts. Photomicrographs and quantification of local cell invasion into muscle tissue (**a**, **b**) or subcutaneous fat (**c**, **d**), by either wild-type or SerpinB2$^{-/-}$ MEF:PDAC tumours. Individual values shown are from five or four animals per group in WT or SerpinB2$^{-/-}$ respectively, with mean ± s.e.m. denoted. Statistical analyses were performed using unpaired *t*-tests. (**e**) uPA enzymatic activity (IU/mg) from either wild-type or SerpinB2$^{-/-}$ MEF:PDAC tumour lysates (bars represent mean ± s.e.m., $n = 3$).

Histological analysis of excised tumours showed a clear role for stromal SerpinB2-mediated regulation of uPA activity in driving local invasion. Tumours formed with wild-type MEFs were largely encapsulated, with well-defined margins and little evidence of invasion into surrounding muscle (Figure 5a) or fat (Figure 5c). In contrast, tumours formed with SerpinB2$^{-/-}$ MEFS had poorly defined margins (Figures 5a and c). Tumour boundaries were compromised, with tumour invasion into both muscle (Figure 5a) and fat (Figure 5c) clearly observed. These qualitative differences are reflected by a significant increase in local invasion score in tumours formed with SerpinB2$^{-/-}$ MEFs compared to wild-type MEFs (Figures 5b and d) using the scoring system described in Supplementary Figure S3. These data clearly show that SerpinB2 inhibits PDAC local invasion, likely via regulation of stromal collagen remodelling.

As the canonical role of SerpinB2 is the specific, rapid inhibition and clearance of cell surface-bound uPA,[19,40–42] this function may also be relevant to the observed effects on PDAC invasion *in vivo*. To this end we measured uPA proteolytic activity in tumour allograft homogenates. The increased local invasion of tumours formed with SerpinB2$^{-/-}$ MEFs was associated with increased uPA proteolytic activity in these tumours (250.4 ± 51.1 IU/mg versus 654.9 ± 136.0 IU/mg in wild-type and SerpinB2$^{-/-}$, respectively; $P < 0.05$) (Figure 5e).

PLAU expression is associated with poorer survival following pancreatectomy

Our observation of increased uPA activity in mixed-cell allograft tumours formed with SerpinB2$^{-/-}$ MEFs is consistent with the well-established role of uPA in invasion and metastasis across a range of cancer types.[15] We therefore examined the association between mRNA expression of the uPA encoding gene, PLAU, and disease-specific survival in a second, independent cohort of patients with resected PDAC (Australian Pancreatic Cancer Genome Initiative (APGI)).[7] Increasing PLAU expression was significantly associated with poorer survival following pancreatectomy (Figures 6a and b; Cox model coefficient 0.387, likelihood ratio $P = 0.00019$, $n = 141$). This corresponds to an approximate doubling of median survival time from diagnosis between the 10th and 90th percentiles for uPA expression. Case-to-case matched analysis of SerpinB2, PLAU and PLAUR mRNA expression in this independent cohort showed that SerpinB2 mRNA levels were at the threshold of detection in many cases (Supplementary Figure S5), consistent with the frequent gene deletion we observed in the UTSW data set (Figure 1). Further, many of the samples with below-threshold SerpinB2 mRNA detection levels have high PLAU and/or PLAUR expression (Supplementary Figure S5), consistent with increased uPA activity in the mixed-cell allografts formed with SerpinB2$^{-/-}$ MEFS.

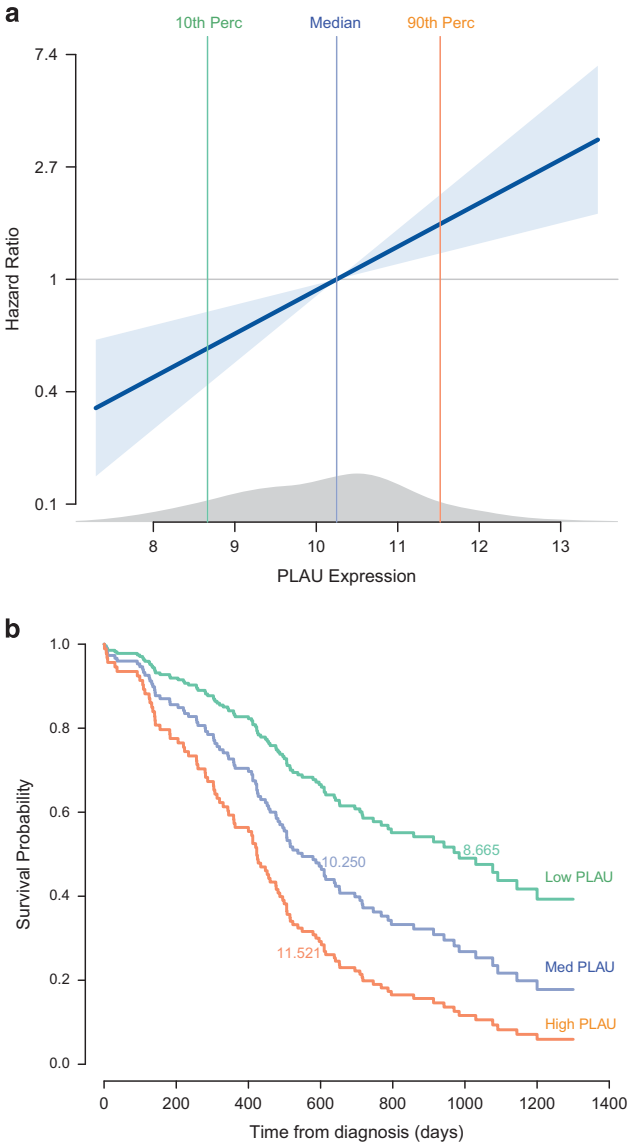

Figure 6. PLAU expression is associated with poor prognosis following pancreatectomy. Hazard ratio (**a**) and overall survival (**b**) in relation to PLAU mRNA expression (log scale) for a cohort of patients with resected PDAC ($n = 141$). Increasing PLAU expression was significantly associated with poor prognosis following pancreatectomy (Cox model coefficient 0.387; likelihood ratio $P = 1.9e\text{-}4$). Standard error of the fit is shown as a light blue band, and the distribution of PLAU expression in the cohort as a grey density distribution. 10th, 50th and 90th percentiles of the PLAU expression distribution are indicated by vertical green, blue, and orange lines, respectively. The Cox model predicted survival curves for these three percentiles of PLAU expression are further illustrated in (**b**).

DISCUSSION

Beyond surgery, current PDAC treatment options are limited and have not substantially improved the survival of patients with unresectable disease over the past 25 years. There is therefore an urgent need for better understanding of this disease to provide new therapeutic strategies to treat advanced disease, as 80% of patients are unsuitable for pancreatectomy.[43] Herein, we identify SerpinB2 as a regulator of PDAC invasion and stromal remodelling, and show that its enzymatic target uPA is a marker of PDAC outcome/survival.

At the genomic level, we observed mutually exclusive alterations of various PAS components in a significant proportion of PDAC cases. The predicted effects of these different alterations are functionally equivalent. That is, deletion of SERPINB2 (18q21.33-q22.1) or the amplification of either its enzyme target PLAU (10q22.2) or enzyme receptor PLAUR (19q13.31), would have the comparable effect of increasing uPA proteolytic capacity. Mutually exclusive genomic alterations within a particular pathway strongly predict a role for that pathway in driving tumorigenesis.[44] Interestingly, amplification of another uPA inhibitor, SERPINE1, frequently occurred in PDAC. Overexpression of SerpinE1 (PAI-1) is often associated with poor prognosis, and uPA and SerpinE1 are among the prognostic markers available in node-negative breast cancer.[15,45,46] Despite being a uPA inhibitor, SerpinE1 overexpression mediates tumour invasion and metastasis through well-characterized secondary interactions with the ECM

component vitronectin and/or endocytosis receptors, which promote cell proliferation and migration.[14] In contrast, SerpinB2 lacks the high affinity endocytosis receptor-binding motif and cannot bind to vitronectin, and thus inhibits and clears uPA protease activity, a key step suppressing invasion and metastasis, without inducing the mitogenic and motogenic signals induced by SerpinE1.[18] We show a strong association between increased PLAU mRNA expression and decreased survival in a large cohort of patients with resectable pancreatic cancer—from over 3 years with low expression to 18 months with high expression. In this respect, the pattern of genomic alterations in PAS components, particularly the frequent loss of SERPINB2, is consistent with a role in PDAC biology.

An important consideration in interpreting genomic data on whole tumour extracts is the relatively low tumour cellularity, high stromal content and related desmoplasia that is characteristic of PDAC.[7,47] Therefore, to understand the role of SerpinB2 in PDAC biology it is critical to consider functional effects in a cell-specific context. Numerous studies have linked stromal expression of SerpinB2 to disease progression in various tumour types, including pancreatic cancer.[15] Collagen matrix contraction in the presence of SerpinB2$^{-/-}$ fibroblasts produced a striking effect on matrix integrity, demonstrating that SerpinB2 regulates fibroblast-mediated contraction and their capacity to efficiently remodel the surrounding matrix. Complementary SHG and SEM analyses of matrices formed by SerpinB2$^{-/-}$ MEFs revealed anisotropic dispersal of collagen I, compared with the isotropic distribution observed in matrices formed with wild-type MEFs.[48,49] These data suggest that SerpinB2 is necessary for fibroblast-dependent manipulation and remodelling of the ECM. This collagen deposition/remodelling phenotype is consistent with an *in vivo* model of liver parasite infection, in which SerpinB2 deficiency resulted in reduced collagen deposition and fibrosis.[50]

We observed significantly decreased movement of SerpinB2$^{-/-}$ MEFs in organotypic culture, and striking differences in cellular protrusion dynamics in these cells, suggesting that the effect of SerpinB2 on matrix remodelling is primarily through a novel role in regulation of fibroblast motility and interactions with the surrounding ECM. Given that the primary biochemical function of extracellular SerpinB2 is inhibition of uPA activity, the potential role of uPA proteolytic activity in mediating the effect of SerpinB2 on collagen matrix remodelling should be considered in future studies. Metalloproteinases (MMPs) are considered more important in the collagen deposition/contraction stage,[51] and many of these do not require uPA for activation.[52] However, *in vivo* evidence for uPA-mediated plasmin(ogen) activation of a number of pro-MMPS including pro-MMP-3, -9 and -13 (which then directly degrade and remodel ECM) has been reported in aneurysm models.[53] It is thus also possible that in the absence of SerpinB2, enhanced uPA activity leads to increased activation of pro-MMPs. An additional or alternative mechanism to explain the effect of SerpinB2 deficiency on collagen remodelling could also be related to differential fibroblast activation states of SerpinB2$^{-/-}$ versus WT MEFs. For example, migratory myofibroblasts play an important role in collagen contraction, ECM turnover and composition.[54]

The major histopathological hallmark of PDAC is the high stromal-to-epithelial ratio associated with fibrosis and desmoplasia.[55] In a mixed allograft model recapitulating this characteristically high stroma:tumour ratio, we observed a clear role for stromal SerpinB2 in modulating both collagen remodelling and local tumour invasion. Mixed cell tumours formed with SerpinB2-deficient MEFs proliferated more and were significantly more invasive, with reduced collagen deposition. Hence, the disrupted stromal architecture induced by SerpinB2 deficiency had a clear effect on PDAC cell invasion *in vivo*. There have been conflicting hypotheses concerning the role of the tumour microenvironment in PDAC.[13,56] Our data show that reduced stromal integrity is associated with tumour growth and local invasion, consistent with other recent studies.[10–14]

Considering that the primary biochemical function of SerpinB2 is as a uPA inhibitor, it is notable that tumours formed with SerpinB2-deficient MEFs had significantly enhanced uPA proteolytic activity compared to those formed with wild-type MEFs. This was associated with significantly increased local invasion in SerpinB2-deficient tumours, suggesting that stromal-derived SerpinB2 may be regulating extracellular or pericellular proteolysis. Together with the observation of frequent loss of SerpinB2 and/or increased uPA/uPAR expression in multiple PDAC cohorts, a potential role for uPA proteolytic activity in disease progression cannot be excluded, and is consistent with our novel clinical data showing an association between uPA expression and survival in PDAC. Clinicopathological data in other solid tumours have also implicated the uPA/SerpinB2 axis in invasion and metastasis. Hence, in this complex and dynamic *in vivo* context, SerpinB2 may have a dual role, regulating both stromal integrity and uPA-dependent PDAC invasion. Further, these findings provide biological support for further investigation of the potential of uPA-targeted therapeutics in pancreatic cancer.

MATERIALS AND METHODS

Gene expression survival analysis

Analysis of alteration frequencies in PAS components across various tumour types (Figure 1) was performed using the cBioPortal for Cancer Genomics.[20,21] Genomic alterations in PDAC (Figure 1) were performed using the UTSW cohort[35] of 109 cases. Outcome data and gene expression measurements for the APGI PDAC cohort[7] (Figure 6 and Supplementary Figure S5) are available from the ICGC DCC (https://dcc.icgc.org/). Gene expression measurements from bulk tumour were made on the Illumina Human HT-12 V4 platform, and were processed using the Bioconductor lumi package (v 2.18.0), using 'bgAdjust.affy' background subtraction, 'vst' transformation and 'quantile' normalization. Outcome data were current at March 2016. The influence of log-expression on disease-specific survival was examined separately for each probe. Martingale residual plots were used to assess functional form, and no departures from linearity were observed. The prognostic significance of each probe was then evaluated by likelihood-ratio tests, comparing a Cox model with probe log-expression as a linear predictor, against a marginal model. The influence of significantly prognostic probes on survival was visualized by plotting the Cox model predicted hazard ratio against probe log-expression, and further illustrated by comparing fitted survival curves corresponding to 10th, 50th and 90th percentiles of probe expression. Multiple testing correction was performed by Holm's method. All data processing was performed in the R environment (version 3.1.1, survival package version 2.37–7).

Cell lines and culture conditions

Primary mouse PDAC cells were derived from tumours harvested from *Pdx1-Cre, LSL-KRas$^{G12D/+}$, LSL-Trp53$^{R172H/+}$* mice[32] and maintained in Dulbecco's modified Eagle's medium supplemented with 10% fetal bovine serum and penicillin/streptomycin 1%. All cell cultures were routinely monitored for absence of mycoplasma contamination using the MycoAlert™ Mycoplasma Detection Kit (Lonza, Switzerland). Spontaneously immortalized wild-type and SerpinB2$^{-/-}$ MEFs were generated and cultured as previously described.[34] Effects of SerpinB2 deficiency on collagen matrix contraction were also confirmed using a second, independently derived set of spontaneously immortalized wild-type and SerpinB2$^{-/-}$ MEF isolates from littermates (Supplementary Figure S4). SerpinB2 status of these cells was confirmed by RT-qPCR (data not shown) and western blot of whole cell lysates (Supplementary Figure S1). Wild-type and SerpinB2$^{-/-}$ cells expressing GFP were generated by viral transduction using VSV-G pseudotyped lentivirus encoding pLV411 vector.[57] Viral particles were packaged using HEK-293 T cells (CRL-3216, ATCC, USA) using standard procedures.[58] GFP-positive MEFs were enriched by sorting with a FACS Vantage instrument (Becton Dickinson, USA).

Organotypic contraction assay

Contraction of collagen I matrices by either wild-type or SerpinB2$^{-/-}$ MEFs was performed as previously described.[30] Briefly, rat-tail tendon collagen was extracted with 0.5 M acetic acid to a concentration of ~2.0 mg/ml. Contraction to a 3D matrix was conducted by embedding quiescent fibroblasts ($1.0–1.5 \times 10^6$ per 12 matrices) into the neutralized collagen I solution. Detached polymerized matrix in 35 mm Petri dishes was then allowed to contract for up to 12 days in complete media (Dulbecco's modified Eagle's medium, supplemented with 10% FCS and 1% penicillin/streptomycin), refreshed every six days.

Histological analysis

Samples were fixed in 10% neutral buffered formalin overnight and processed using the Leica Peloris Dual Retort tissue processor (Germany). Histological staining was performed on 4 µm sections deparaffinized in xylene and rehydrated using graded ethanol washes. Haematoxylin and eosin and picrosirius red (Polysciences, USA, #24901-250) staining were performed on a Leica Autostainer XL. Immunohistochemistry was performed using the Leica Bond RX system. Refer to Supplementary Table S1 for antibody details. For scoring of invasive index, migration modality, cell cluster and immunohistochemistry staining, three representative images per condition were acquired using a bright field microscope (Leica DM4000).

For immunofluorescence analysis, pancreatic tumour allograft cryosections (4 µm) were fixed in 100% acetone for 10 min at − 20 °C and air-dried. Rehydrated sections were blocked and processed with antibodies as described in Supplementary Table S1. Slides were then mounted with Vectashield containing DAPI (Vector) and cells imaged using a Leica DMI 6000 SP8 laser scanning confocal fluorescence microscope. Staining specificity was shown with isotype controls.

Second harmonic generation (SHG) imaging analysis

Second harmonic generation imaging is a label-free, two photon microscopy technique used to image fibrillar, crosslinked collagen in tissues. SHG is a photonic process in which two low energy photons are converted into one photon with twice the incident frequency of the excitation source.[59] SHG signal was acquired through an 80-µm z-stack in fixed collagen matrices and through a 20-µm z-stack in tumour sections using a ×20 0.95 NA water immersion objective on an inverted Nikon TE-2000 microscope body. The excitation source was a Ti:Sapphire femtosecond laser cavity (Coherent Chameleon Ultra II, USA), coupled to a LaVision Biotec Trim-scope scan-head. 840 ± 20 nm excitation wavelength/420 ± 10 nm emission wavelength were used to collect SHG signal from collagen I fibres. ImageJ (NIH, USA) was used to extract SHG signal intensity per optical slice.

Tracking of fibroblast movements in collagen I matrices

GFP-tagged wild-type and SerpinB2$^{-/-}$ MEFs were detected using a 920-nm excitation wavelength and SHG signal derived from collagen fibres was collected as described above on unfixed matrices. Cells were imaged in the central part of the matrix (typically where the matrix was thickest for wild-type MEF matrices) to avoid any potential edge effects. Fibroblast motility within matrices was tracked by recording cell position (X,Y) versus time with Imaris 8.0 (Bitplane, USA), using the built-in spots and isosurface tracking routines (130–160 cells were tracked per experiment). Cells were excluded from analysis if the cell centroid moved less than one cell diameter, or exhibited a blebbing phenotype, over the 14-h timecourse. Furthermore, cells displaying oscillations or shape changes were excluded from the analysis to minimize artefacts associated with automated analysis. Using MATLAB (Mathworks, USA) the X,Y coordinates, with the first coordinates set to 0,0, were plotted for one representative experiment.

Scanning electron microscopy

Fixed specimens were sliced and clamped in a cooling chamber consisting of a 25 mm × 10 mm brass block with a sample chamber groove. The brass holder containing each sample was plunged into a bath of liquid nitrogen for 40–45 s and then fractured with a liquid nitrogen cooled blade, to expose a cross-section surface that was flush with the surface of the brass block. The cooled holder with the fractured sample was then inserted into a JEOL 6490LV scanning electron microscope equipped with a secondary electron detector and a backscattered electron detector (scintillator type) using acceleration voltages between 10 and 20 kV. Images were recorded with an integrated JEOL digital image acquisition system.

Mixed cell allograft model

7.5×10^5 MEFs (wild-type or SerpinB2$^{-/-}$) were mixed with 2.5×10^5 PDAC cells (1×10^6 cells in total at a 3:1 MEF:PDAC ratio) and injected subcutaneously into the rear flank of BALB/c-Fox1nuAusb mice (5 per group). Tumour volume was quantified using a digital vernier caliper and calculated as: width × width × length/2.[60] Mice were monitored daily in compliance with the Garvan/St Vincent's Hospital Animal Experimentation and Ethics Committee guidelines (approval #13/17). Mice were anesthetized 7 days post injection and tumours were imaged using an IVIS system.

Cell invasion into local tissue (subcutaneous fat, muscle and skin) was analysed by histoscore on 4 µm H&E stained sections. Local invasion was quantified as shown in Supplementary Figure S3, and scored blind by three separate researchers.

Urokinase activity assays in tumour lysates were performed as previously described.[61] Briefly, tumours were homogenized in 10 mM Tris, pH 8.0, 0.15 M NaCl, 1% Triton X-100, and lysates diluted in 100 µl reaction buffer (20 mM HEPES, pH 7.6, 100 mM NaCl, 0.5 mM EDTA, 0.01% (v/v) Tween-20) containing 0.25 mM uPA fluorogenic substrate (Z-Gly-Gly-Arg-AMC—Chemicon, USA). Fluorescence was measured kinetically using a POLAstar plate reader (OMEGA) and activity determined against a murine uPA standard.

Statistical analyses

Differences in the mean of two groups were analysed by an unpaired *t*-test. Comparisons of more than two groups were made by a one-way (or two-way) ANOVA with post hoc Holm–Sidak analysis for pairwise comparisons and comparisons versus control. P values < 0.05 were considered statistically significant. Data and statistical analyses were performed using GraphPad Prism (version 6.0, USA).

CONFLICT OF INTEREST

The authors declare no conflict of interest.

ACKNOWLEDGEMENTS

This work was supported by funding from the National Health and Medical Research Council (DS, PT, MP); Cancer Institute NSW (DS, PT, MR); Cancer Council NSW (PT, MP); Tour De Cure (PT); Cure Cancer Australia Foundation (KLV); Australian Research Council (PT); University of Wollongong (MR) and Illawarra Health and Medical Research Institute (MR); Mostyn Family Foundation and Guest Family Fellowship (DS) and Garvan Research Foundation (DS, PT), Sydney Catalyst (CV). PT is a recipient of the Lens Ainsworth Pancreatic Cancer Fellowship, KLV was a recipient of a University of Wollongong Vice Chancellor's Fellowship. NLH is supported by an Australian Postgraduate Award PhD scholarship. The authors acknowledge use of the facilities and the assistance of Dr Tony Romeo and Dr Mitchell Nancarrow at the UOW Electron Microscopy Centre, the assistance of Alice Boulghourjian and Anaiis Zaratzian at The Kinghorn Cancer Centre Histopathology facility, and other technical assistance of Elahe Minaei at Illawarra Health and Medical Research Institute.

REFERENCES

1 Siegel RL, Miller KD, Jemal A. Cancer statistics, 2016. *CA Cancer J Clin* 2016; **66**: 7–30.
2 Neesse A, Michl P, Frese KK, Feig C, Cook N, Jacobetz MA *et al*. Stromal biology and therapy in pancreatic cancer. *Gut* 2011; **60**: 861–868.
3 Goldstein D, El-Maraghi RH, Hammel P, Heinemann V, Kunzmann V, Sastre J *et al*. nab-Paclitaxel plus gemcitabine for metastatic pancreatic cancer: long-term survival from a phase III trial. *J Natl Cancer Inst* 2015; **107**: dju413.
4 Von Hoff DD, Ervin T, Arena FP, Chiorean EG, Infante J, Moore M *et al*. Increased survival in pancreatic cancer with nab-paclitaxel plus gemcitabine. *N Engl J Med* 2013; **369**: 1691–1703.
5 Rowe RG, Sheikh R, Weiss SJ, Walsh N, Clynes M, O'Connor R *et al*. Challenges of drug resistance in the management of pancreatic cancer. *Cancer Epidemiol Biomarkers Prevent* 2000; **9**: 1647–1661.
6 Bailey P, Chang DK, Nones K, Johns AL, Patch A-M, Gingras M-C *et al*. Genomic analyses identify molecular subtypes of pancreatic cancer. *Nature* 2016; **531**: 47–52.

7 Biankin AV, Waddell N, Kassahn KS, Gingras M-C, Muthuswamy LB, Johns AL *et al.* Pancreatic cancer genomes reveal aberrations in axon guidance pathway genes. *Nature* 2012; **491**: 399–405.
8 Waddell N, Pajic M, Patch A-M, Chang DK, Kassahn KS, Bailey P *et al.* Whole genomes redefine the mutational landscape of pancreatic cancer. *Nature* 2015; **518**: 495–501.
9 Kalluri R, Zeisberg M. Fibroblasts in cancer. *Nat Rev Cancer* 2006; **6**: 392–401.
10 Lee JJ, Perera RM, Wang H, Wu DC, Liu XS, Han S *et al.* Stromal response to Hedgehog signaling restrains pancreatic cancer progression. *Proc Natl Acad Sci USA* 2014; **111**: E3091–E3100.
11 Lee J, Condello S, Yakubov B, Emerson R, Caperell-Grant A, Hitomi K *et al.* Tissue transglutaminase mediated tumor-stroma interaction promotes pancreatic cancer progression. *Clin Cancer Res* 2015; **21**: 4482–4493.
12 Rhim AD, Oberstein PE, Thomas DH, Mirek ET, Palermo CF, Sastra SA *et al.* Stromal elements act to restrain, rather than support, pancreatic ductal adenocarcinoma. *Cancer Cell* 2014; **25**: 735–747.
13 Gore J, Korc M. Pancreatic cancer stroma: friend or foe? *Cancer Cell* 2014; **25**: 711–712.
14 Ozdemir BC, Hensel J, Secondini C, Wetterwald A, Schwaninger R, Fleischmann A *et al.* The molecular signature of the stroma response in prostate cancer-induced osteoblastic bone metastasis highlights expansion of hematopoietic and prostate epithelial stem cell niches. *PLoS ONE* 2014; **9**: e114530.
15 Croucher DR, Saunders DN, Lobov S, Ranson M. Revisiting the biological roles of PAI2 (SERPINB2) in cancer. *Nat Rev Cancer* 2008; **8**: 535–545.
16 LeBeau AM, Sevillano N, Markham K, Winter MB, Murphy ST, Hostetter DR *et al.* Imaging active urokinase plasminogen activator in prostate cancer. *Cancer Res* 2015; **75**: 1225–1235.
17 Ulisse S, Baldini E, Sorrenti S, D'Armiento M. The urokinase plasminogen activator system: a target for anti-cancer therapy. *Curr Cancer Drug Targets* 2009; **9**: 32–71.
18 Smith HW, Marshall CJ. Regulation of cell signalling by uPAR. *Nat Rev Mol Cell Biol* 2010; **11**: 23–36.
19 Cochran BJ, Croucher DR, Lobov S, Saunders DN, Ranson M. Dependence on endocytic receptor binding via a minimal binding motif underlies the differential prognostic profiles of SerpinE1 and SerpinB2 in cancer. *J Biol Chem* 2011; **286**: 24467–24475.
20 Cerami E, Gao J, Dogrusoz U, Gross BE, Sumer SO, Aksoy BA *et al.* The cBio cancer genomics portal: an open platform for exploring multidimensional cancer genomics data. *Cancer Discov* 2012; **2**: 401–404.
21 Gao J, Aksoy BA, Dogrusoz U, Dresdner G, Gross B, Sumer SO *et al.* Integrative analysis of complex cancer genomics and clinical profiles using the cBioPortal. *Sci Signal* 2013; **6**: pl1–pl1.
22 Shiomi H, Eguchi Y, Tani T, Kodama M, Hattori T. Cellular distribution and clinical value of urokinase-type plasminogen activator, its receptor, and plasminogen activator inhibitor-2 in esophageal squamous cell carcinoma. *Am J Pathol* 2000; **156**: 567–575.
23 Finak G, Bertos N, Pepin F, Sadekova S, Souleimanova M, Zhao H *et al.* Stromal gene expression predicts clinical outcome in breast cancer. *Nat Med* 2008; **14**: 518–527.
24 Smith R, Xue A, Gill A, Scarlett C, Saxby A, Clarkson A *et al.* High expression of plasminogen activator inhibitor-2 (PAI-2) is a predictor of improved survival in patients with pancreatic adenocarcinoma. *World J Surg* 2007; **31**: 493–502.
25 Takeuchi Y, Nakao A, Harada A, Nonami T, Fukatsu T, Takagi H. Expression of plasminogen activators and their inhibitors in human pancreatic carcinoma: immunohistochemical study. *Am J Gastroenterol* 1993; **88**: 1928–1933.
26 Xue A, Scarlett CJ, Jackson CJ, Allen BJ, Smith RC. Prognostic significance of growth factors and the urokinase-type plasminogen activator system in pancreatic ductal adenocarcinoma. *Pancreas* 2008; **36**: 160–167.
27 Herrmann D, Conway JRW, Vennin C, Magenau A, Hughes WE, Morton JP *et al.* Three-dimensional cancer models mimic cell-matrix interactions in the tumour microenvironment. *Carcinogenesis* 2014; **35**: 1671–1679.
28 Nurmenniemi S, Sinikumpu T, Alahuhta I, Salo S, Sutinen M, Santala M *et al.* A novel organotypic model mimics the tumor microenvironment. *Am J Pathol* 2009; **175**: 1281–1291.
29 Nyström ML, Thomas GJ, Stone M, Mackenzie IC, Hart IR, Marshall JF. Development of a quantitative method to analyse tumour cell invasion in organotypic culture. *J Pathol* 2005; **205**: 468–475.
30 Timpson P, Mcghee EJ, Erami Z, Nobis M, Quinn JA, Edward M *et al.* Organotypic collagen I assay: a malleable platform to assess cell behaviour in a 3-dimensional context. *J Vis Exp* 2011; **56**: e3089.
31 Hingorani SR, Wang L, Multani AS, Combs C, Deramaudt TB, Hruban RH *et al.* Trp53R172H and KrasG12D cooperate to promote chromosomal instability and widely metastatic pancreatic ductal adenocarcinoma in mice. *Cancer Cell* 2005; **7**: 469–483.
32 Morton JP, Timpson P, Karim SA, Ridgway RA, Athineos D, Doyle B *et al.* Mutant p53 drives metastasis and overcomes growth arrest/senescence in pancreatic cancer. *Proc Natl Acad Sci USA* 2010; **107**: 246–251.
33 Hingorani SR, Petricoin EF, Maitra A, Rajapakse V, King C, Jacobetz MA *et al.* Preinvasive and invasive ductal pancreatic cancer and its early detection in the mouse. *Cancer Cell* 2003; **4**: 437–450.
34 Lee JA, Yerbury JJ, Farrawell N, Shearer RF, Constantinescu P, Hatters DM *et al.* SerpinB2 (PAI-2) modulates proteostasis via binding misfolded proteins and promotion of cytoprotective inclusion formation. *PLoS ONE* 2015; **10**: e0130136.
35 Witkiewicz AK, McMillan EA, Balaji U, Baek G, Lin WC, Mansour J *et al.* Whole-exome sequencing of pancreatic cancer defines genetic diversity and therapeutic targets. *Nat Commun* 2015; **6**: 6744.
36 Boyd ZS, Raja R, Johnson S, Eberhard DA, Lackner MR. A tumor sorting protocol that enables enrichment of pancreatic adenocarcinoma cells and facilitation of genetic analyses. *J Mol Diagn: JMD* 2009; **11**: 290–297.
37 Seymour AB, Hruban RH, Redston M, Caldas C, Powell SM, Kinzler KW *et al.* Allelotype of pancreatic adenocarcinoma. *Cancer Res* 1994; **54**: 2761–2764.
38 Shekouh AR, Thompson CC, Prime W, Campbell F, Hamlett J, Herrington CS *et al.* Application of laser capture microdissection combined with two-dimensional electrophoresis for the discovery of differentially regulated proteins in pancreatic ductal adenocarcinoma. *Proteomics* 2003; **3**: 1988–2001.
39 Gaggioli C, Hooper S, Hidalgo-Carcedo C, Grosse R, Marshall JF, Harrington K *et al.* Fibroblast-led collective invasion of carcinoma cells with differing roles for RhoGTPases in leading and following cells. *Nat Cell Biol* 2007; **9**: 1392–1400.
40 Al-Ejeh F, Croucher D, Ranson M. Kinetic analysis of plasminogen activator inhibitor type-2: urokinase complex formation and subsequent internalisation by carcinoma cell lines. *Exp Cell Res* 2004; **297**: 259–271.
41 Croucher D, Saunders DN, Ranson M. The urokinase/PAI-2 complex: a new high affinity ligand for the endocytosis receptor low density lipoprotein receptor-related protein. *J Biol Chem* 2006; **281**: 10206–10213.
42 Croucher DR, Saunders DN, Stillfried GE, Ranson M. A structural basis for differential cell signalling by PAI-1 and PAI-2 in breast cancer cells. *Biochem J* 2007; **408**: 203–210.
43 Garrido-Laguna I, Hidalgo M. Pancreatic cancer: from state-of-the-art treatments to promising novel therapies. *Nat Rev Clin Oncol* 2015; **12**: 319–334.
44 Babur Ö, Gönen M, Aksoy BA, Schultz N, Ciriello G, Sander C *et al.* Systematic identification of cancer driving signaling pathways based on mutual exclusivity of genomic alterations. *Genome Biol* 2015; **16**: 45.
45 Duffy MJ, McGowan PM, Harbeck N, Thomssen C, Schmitt M. uPA and PAI-1 as biomarkers in breast cancer: validated for clinical use in level-of-evidence-1 studies. *Breast Cancer Res* 2014; **16**: 428.
46 Harris L, Fritsche H, Mennel R, Norton L, Ravdin P, Taube S *et al.* American Society of Clinical Oncology 2007 update of recommendations for the use of tumor markers in breast cancer. *J Clin Oncol* 2007; **25**: 5287–5312.
47 Mahadevan D, Von Hoff DD. Tumor-stroma interactions in pancreatic ductal adenocarcinoma. *Mol Cancer Ther* 2007; **6**: 1186–1197.
48 Condeelis J, Segall JE. Intravital imaging of cell movement in tumours. *Nat Rev Cancer* 2003; **3**: 921–930.
49 Nobis M, McGhee EJ, Morton JP, Schwarz JP, Karim SA, Quinn J *et al.* Intravital FLIM-FRET imaging reveals dasatinib-induced spatial control of Src in pancreatic cancer. *Cancer Res* 2013; **73**: 4674–4686.
50 Schroder WA, Gardner J, Le TT, Duke M, Burke ML, JONES MK *et al.* SerpinB2 deficiency modulates Th1/Th2 responses after schistosome infection. *Parasite Immunol* 2010; **32**: 764–768.
51 Telgenhoff D, Shroot B. Cellular senescence mechanisms in chronic wound healing. *Cell Death Differ* 2005; **12**: 695–698.
52 Kessenbrock K, Plaks V, Werb Z. Matrix metalloproteinases: regulators of the tumor microenvironment. *Cell* 2010; **141**: 52–67.
53 Carmeliet P, Moons L, Lijnen R, Baes M, Lemaitre V, Tipping P *et al.* Urokinase-generated plasmin activates matrix metalloproteinases during aneurysm formation. *Nat Genet* 1997; **17**: 439–444.
54 Hinz B. Myofibroblasts. *Exp Eye Res* 2016; **142**: 56–70.
55 Li J, Wientjes MG, Au JL-S. Pancreatic cancer: pathobiology, treatment options, and drug delivery. *AAPS J* 2010; **12**: 223–232.
56 Neesse A, Algül H, Tuveson DA, Gress TM. Stromal biology and therapy in pancreatic cancer: a changing paradigm. *Gut* 2015; **64**: 1476–1484.
57 Barry SC, Harder B, Brzezinski M, Flint LY, Seppen J, Osborne WR. Lentivirus vectors encoding both central polypurine tract and posttranscriptional regulatory element provide enhanced transduction and transgene expression. *Hum Gene Ther* 2001; **12**: 1103–1108.
58 Shearer RF, Saunders DN. Experimental design for stable genetic manipulation in mammalian cell lines: lentivirus and alternatives. *Genes Cells* 2015; **20**: 1–10.

59 Cicchi R, Kapsokalyvas D, De Giorgi V, Maio V, Van Wiechen A, Massi D *et al*. Scoring of collagen organization in healthy and diseased human dermis by multiphoton microscopy. *J Biophotonics* 2010; **3**: 34–43.

60 Stutchbury TK, Al-Ejeh F, Stillfried GE, Croucher DR, Andrews J, Irving D *et al*. Preclinical evaluation of 213Bi-labeled plasminogen activator inhibitor type 2 in an orthotopic murine xenogenic model of human breast carcinoma. *Mol Cancer Ther* 2007; **6**: 203–212.

61 Cochran BJ, Gunawardhana LP, Vine KL, Lee JA, Lobov S, Ranson M. The CD-loop of PAI-2 (SERPINB2) is redundant in the targeting, inhibition and clearance of cell surface uPA activity. *BMC Biotechnol* 2009; **9**: 43.

Supplementary Information accompanies this paper on the Oncogene website (http://www.nature.com/onc)